

Molecular and biochemical characterization of human galactokinase and its small molecule inhibitors

M. Tang^a, K. Wierenga^b, L.J. Elsas^a, K. Lai^{a,c,*}

^a Department of Biochemistry and Molecular Biology, University of Miami Miller School of Medicine, USA

^b Section of Genetics, Department of Pediatrics, University of Oklahoma Health Sciences Center, USA

^c Division of Medical Genetics, Department of Pediatrics, University of Utah School of Medicine, USA

ARTICLE INFO

Article history:

Received 26 April 2010

Received in revised form 20 July 2010

Accepted 30 July 2010

Available online 7 August 2010

Keywords:

Inborn error of metabolism

Galactokinase

Galactose-1-phosphate

Small molecule enzyme inhibitors

GHMP kinases

Drug discovery

ABSTRACT

Human galactokinase (GALK) is the first enzyme in the Leloir pathway, converting α -D-galactose into galactose-1-phosphate (Gal-1-P). Recently, there is increasing interest in targeting GALK as a novel therapy to ameliorate the disease manifestations in patients with Classic Galactosemia as it would, in combination with (ga-)lactose restriction reduce accumulation of Gal-1-P, a cytotoxic agent. Previously, we identified 34 small molecule compounds that inhibited GALK *in vitro* using experimental high-throughput screening. In order to isolate useful lead compounds, we characterized these hits with regards to their kinase selectivity profiles, potency and capability to reduce Gal-1-P accumulation in patient cell lines, and their modes of action. We found that the majority of these compounds had IC_{50} s ranging from 0.7 μ M to 33.3 μ M. When tested against other members of the GHMP kinase family, three compounds (1, 4, and 24) selectively inhibited GALK with high potency. Through alignment of GALK and mevalonate kinase (MVK) crystal structures, we identified that eight amino acid residues and an L1 loop were different within the ATP-binding pockets of these two closely related kinases. By site-directed mutagenesis experiments, we identified one amino acid residue required for the inhibitory function of two of the three selective compounds. Based on these results, we generated binding models of these two compounds using a high-precision docking program. Compounds 4 and 24 inhibited GALK in a mixed model, while compound 1 exhibited parabolic competitive inhibition. Most importantly, using cells from galactosemic patients we found that selected compounds lowered Gal-1-P concentrations.

© 2010 Elsevier Ireland Ltd. All rights reserved.

1. Introduction

In all living cells, the metabolism of α -D-galactose requires its conversion to galactose-1-phosphate (Gal-1-P) by the enzyme galactokinase (GALK). In the presence of galactose-1-phosphate uridylyltransferase (GALT), Gal-1-P will react with UDP-Glucose to form UDP-Galactose and glucose-1-phosphate [1]. Classic Galactosemia is an autosomal recessive metabolic disorder caused by the deficiency of galactose-1-phosphate uridylyltransferase (GALT) [2], consequently leading to accumulation of Gal-1-P and deficiency of UDP-Galactose and UDP-Glucose in patient cells [3,4]. If untreated, Classic Galactosemia can result in severe disease in the newborn period, including liver failure, coagulopathy, coma, and death [5–7]. Classic Galactosemia is included in newborn screening panels in the United States, since a galactose-restricted diet

prevents the neonatal lethality of this disorder [8]. However, many well-treated newborns continue to develop complications such as premature ovarian insufficiency (POI), ataxia, speech dyspraxia, and mental retardation [7]. The causes of these organ-specific complications remain unknown, but there is a strong association with the intracellular accumulation of Gal-1-P. But what is the source of Gal-1-P in these patients with Classic Galactosemia if they limit their galactose intake? Recent studies have shown that the patients on a galactose-restricted diet are never really “galactose-free”. A significant amount of galactose is found in non-dairy foodstuffs such as vegetables and fruits [9,10]. More importantly, galactose is produced endogenously from the natural turnover of glycolipids and glycoproteins [11]. Using isotopic labeling, Berry et al. demonstrated that a 50 kg adult male could produce up to 2 grams of galactose per day [11,12]. Once galactose is formed intracellularly, it is converted to Gal-1-P by GALK and in GALT-deficient patients' cells, Gal-1-P is concentrated more than one order of magnitude above normal, even with strict adherence to a galactose-restricted diet. Accumulation of Gal-1-P is regarded as a major, if not sole, factor for the chronic complications seen in patients with Classic Galactosemia, as suggested by both clinical observa-

* Corresponding author at: Division of Medical Genetics, Department of Pediatrics, University of Utah School of Medicine, 50 N. Mario Capecchi Drive, SOM Room 2C412, Salt Lake City, UT 84132, USA.

E-mail address: kent.lai@hsc.utah.edu (K. Lai).

tion and experimental results from the yeast models. First, patients with inherited deficiency of GALK, who do not accumulate Gal-1-P, do not experience the brain and ovary complications seen in GALT-deficient patients [13–15]. Second, while *gal7* (i.e., GALT-deficient) mutant yeast stops growing upon galactose challenge, a *gal7 gal1* double mutant strain (i.e., GALT- and GALK-deficient) is no longer sensitive to galactose [16,17]. Based on these observations, in conjunction with dietary therapy, inhibiting GALK activity with a safe small molecule inhibitor might prevent the sequelae of chronic Gal-1-P exposure in patients with Classic Galactosemia. Previously, we identified 34 GALK inhibitors from experimental high-throughput screening of 50,000 small molecule compounds with diverse structural scaffolds [18]. In this study, we define the selectivity, sensitivity, toxicity, *in vitro* kinetics and *in vivo* effects of selected inhibitors for GALK.

Although GALK phosphorylates galactose, a six-carbon monosaccharide, this human enzyme does not belong to the sugar kinase family. It is, in fact, an archetype of the GHMP kinase family (GHMP: galactokinase, homoserine kinase, mevalonate kinase and phosphomevalonate kinase) [19,20]. Proteins belonging to this family have a different structure compared to other kinase families. All members of the GHMP kinase family have three conserved motifs (I, II and III). Motif II is the most conserved motif with a typical sequence of Pro-X-X-Gly-Leu-X-Ser-Ser-Ala and is involved in nucleotide binding [19]. The characterization of selective GALK inhibitors can therefore offer novel insights into the structural biology of the GHMP kinases.

2. Materials and methods

2.1. Enzymes over-expression and purification

Cloning, over-expression and purification of human GALK were performed as described [18]. The plasmid containing human mevalonate kinase (MVK) cDNA was purchased from *Invitrogen* and the MVK cDNA was later sub-cloned into bacterial expression vector pET-21d. The expression plasmid clone of *Methanococcus jannaschii* homoserine kinase (HSK) was kindly shared by Dr. Hong Zhang, UT Southwestern Medical Center. The 4-diphosphocytidyl-2C-methyl-D-erythritol (CDP-ME) kinase gene from *Escherichia coli* DH5 α was isolated by PCR in our laboratory and was subsequently sub-cloned into the vector pET-21d. The expression and purification protocols for MVK, HSK and CDP-ME kinase were the same as described for human GALK except there was no galactose in the purification buffers. Glucokinase (cat. #G8887) from *Bacillus stearothermophilus* and hexokinase (cat. #H4502) from *Saccharomyces cerevisiae* were purchased from *Sigma–Aldrich* (St. Louis, MO).

2.2. Site-directed mutagenesis of human GALK cDNA

Primers for site-directed mutagenesis of human GALK cDNA are listed in Table 1. The loop mutation primers that replace the larger L1 loop of GALK into the smaller L1 loop of MVK are included. Using these primers, we introduced the mutations into the wild-type GALK cDNA sequence in pET-21d with QuickChange II Site-directed Mutagenesis Kit (cat. #200523, *Stratagene* (La Jolla, CA)). The introduced sequence changes were confirmed by direct DNA sequencing and the mutated proteins were expressed and purified as mentioned above.

2.3. Enzyme activity assays and inhibition kinetic studies

The IC₅₀ of all compounds were tested with the same two-step ATP-depletion assay for GALK developed with the Kinase-Glo™ reagent (*Promega*, Madison, WI) as described previously [18]. An alternative assay, the pyruvate kinase (PK)/lactate dehydrogenase

(LDH)-coupled assay, which measures the steady-state velocity of the reaction, was also employed to determine the IC₅₀ of compounds and the modes of inhibition. IC₅₀ values were determined from normalized data from both assays using the values obtained for the corresponding controls (i.e., no inhibitor) as 100%. These data were fitted with a standard dose-response inhibition model using *GraphPad Prism 5.01* software (*GraphPad Software, Inc.*, La Jolla, CA), and a log[inhibitor] vs. normalized response model, $y = 100/[1 + 10^{(x - \log IC_{50})}]$, was established for each inhibitor. The models demonstrated adequate fit, with R^2 values of all curves greater than 0.90.

For kinetic analyses of the GALK inhibitors, either galactose or ATP was held in excess while the other was changed under different inhibitor concentrations. The velocity of the reaction was measured by monitoring the change of absorbance at 340 nm, and was plotted against the substrate concentration, then the curve was fit to the equation $V = V_M^{app} S / (K_M^{app} + S)$ by *Sigma Plot 10.0* (*Systat Software, Inc.*, San Jose, CA), where V was the measured reaction velocity, S was the substrate concentration, V_M^{app} was the apparent V_M and K_M^{app} was the apparent K_M . Then an inhibition pattern was assigned based on plotting $1/V_M^{app}$ against the inhibitor concentration and K_M^{app}/V_M^{app} or K_M^{app} against the inhibitor concentration.

2.4. Cell culture, compounds toxicity assessment and measurement of Gal-1-P accumulation in cultured cells

Primary fibroblasts and SV40-transformed fibroblasts derived from GALT-deficient patients were maintained in galactose-free DMEM medium supplemented with 10% fetal bovine serum (FBS). For primary fibroblasts, only the ones less than 32 passages were used for the experiments, but for transformed fibroblasts there was no such limitation.

Compounds were incubated with primary fibroblasts at concentration of 10 μ M, 50 μ M and 100 μ M for 3 days, and then the cellular toxicity of the compounds was evaluated by estimating the cell survival ratio under light microscope.

Before galactose challenge, inhibitors were added to the medium at designated concentrations and incubated at 37°C for 2–4 h. Then galactose was added to reach 0.05% in the medium. After 4 h of challenge, cells were collected and washed with PBS twice. Then the cells were disrupted in 300 μ l of ice cold hypotonic buffer containing 25 mM Tris–HCl (pH 7.4), 25 mM NaCl, 0.5 mM EDTA and protease inhibitor cocktail (*Roche*, cat. # 11 697 498 001). The lysates were passed five times through a 30 gauge needle and centrifuged for 20 min at 16,000 \times g and 4°C. A small portion of supernatant was saved for protein concentration measurement. Gal-1-P level was measured using the methods previously described [21]. The Gal-1-P concentration was normalized to protein concentration.

2.5. Molecular docking experiments and crystal structure alignment

All experiments of docking compounds to the human GALK crystal structure were performed using GLIDE docking software from *Schrodinger* (GLIDE version 5.0, *Schrodinger*, New York) [22–24]. C subunit of human GALK crystal structure 1wu0 was prepared for the docking through *Schrodinger* Maestro protein preparation wizard. First, all the water and metal molecules were removed and bond orders were assigned, necessary hydrogen was added. After the hydrogen bond assignment was optimized, the whole structure was minimized. Then the docking grid was generated on the prepared structure. Two grids were prepared: one centered at the AMPPNP and the other at the galactose moiety in the crystal structure. The compound structures were prepared with Maestro

Table 3Comparing IC₅₀s of inhibitors to galactokinase (GALK), mevalonate kinase (MVK), homoserine kinase (HSK), CDP-ME kinase, glucokinase and hexokinase.

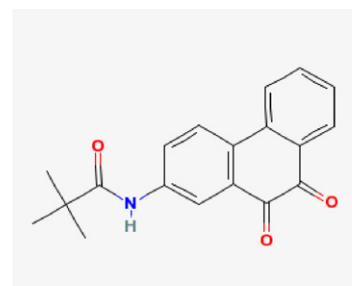
	GALK (μM)	MVK (μM)	HSK (μM)	CDP-ME kinase(μM)	Glucokinase/ hexokinase (μM)		GALK (μM)	MVK (μM)	HSK (μM)	CDP-ME kinase (μM)	Glucokinase/ hexokinase (μM)
1	0.7	>60	>60	>60	>60	18	12.5	23	>60	>60	>60
3	10.5	24.5	>60	>60	>60	20	25	13	>60	5.5	>60
4	1.5	>60	>60	>60	>60	21	18.5	15	>60	5.5	>60
5	12	20	>60	18	>60	22	30	21.3	>60	>60	>60
6	16.5	>60	>60	>60	>60	23	11.5	>60	>60	>60	>60
8	24	25.2	>60	5	>60	24	6.3	>60	>60	>60	>60
9	5.2	8.2	>60	11	>60	26	19.3	11.5	>60	>60	>60
10	6.5	10.3	15.8	>60	>60	27	32	30	>60	>60	>60
11	33.3	40	>60	>60	>60	28	20	21	>60	>60	>60
13	33.3	20	>60	17	>60	30	21.1	14.5	>60	>60	Weak inhibition for Glucokinase
14	27.1	16	>60	>60	>60	31	21	18.5	>60	>60	>60
16	30	40	>60	Not tested	>60	32	20.3	>60	>60	>60	>60
17	12.1	15.2	>60	28	>60						

Note: Compounds were test against mevalonate kinase (MVK), homoserine kinase (HSK), CDP-ME kinase, glucokinase and hexokinase, and IC₅₀s are shown here. IC₅₀s for GALK also listed.

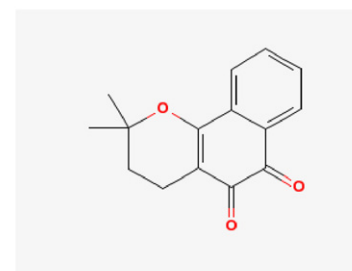
30 inhibited glucokinase weakly (IC₅₀ > 60 μM), but not hexokinase. When we tested the GALK inhibitors against other three GHMP kinases, we found a significant number of them also inhibited human MVK with IC₅₀s similar to that of GALK (Table 3). Four compounds weakly inhibited HSK (IC₅₀s > 60 μM) and eight inhibited bacterial CDP-ME kinase. However, six compounds (1, 4, 6, 23, 24, and 32) had no detectable inhibition against any of the tested GHMP kinases at a concentration up to 60 μM, thus indicating that the unique selectivity of these six inhibitors against human GALK. Based on both potency and selectivity, we chose compound 1, 4, and 24 for further investigation (Fig. 1). Although compound 32 is selective and more importantly, less toxic, it could not be re-synthesized in large quantity, which made further investigation impossible.

3.3. Site-directed mutagenesis of human GALK

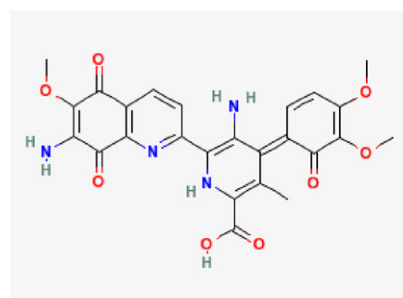
One interesting observation is that except for the six kinase inhibitors mentioned above, the other compounds inhibited both GALK and MVK with similar potency. On the other hand, the other two GHMP kinases (i.e., HSK and CDP-ME kinase) cross-reacted with fewer GALK inhibitors. Based on this observation, we hypothesized that GALK shared more structural similarity with MVK than with the two other GHMP kinases. To test this hypothesis, we aligned the protein sequences of human MVK and *M. jannaschii* HSK to that of the human GALK separately with ClustalW2 [25]. Human GALK and MVK shared 70 identical residues and 69 conserved residues; for HSK, only 56 residues were identical to those of GALK and 67 residues were conserved. We then aligned the crystal structures of human MVK and *M. jannaschii* HSK separately to the crystal structure of human GALK (Fig. 2a and b). As shown in Fig. 2a, the ATP-binding site of GALK aligned well with that of MVK, except the L1 loop of GALK (red arrow) was larger than that of MVK (blue arrow) and covered a larger area. Note that the ATP (MVK) and the AMPPNP (GALK) co-crystallized with these enzymes were proximal to each other. However, as shown in Fig. 2b, when the L1 loop (blue arrow) of GALK was compared to the L1 loop of HSK (blue arrow), the L1 loop of HSK was shifted down and the structures are different. The L1 loop of HSK was closer to the αC helix as well as the adjacent β3 sheet as compared with GALK. These changes led to a narrower binding pocket for the adenine of ADP in HSK, which might explain why the ADP adopted a different binding pose for HSK. In fact, the adenine flipped almost 180° away in the HSK crystal structure.



Compound 1



Compound 4



Compound 24

Fig. 1. Structure of three compounds specifically inhibit human GALK.

To explain why the six compounds selectively inhibited human GALK but not human MVK, we compared the crystal structures of these two kinases in more detail, focusing on their ATP-binding pockets. Except for the L1 loop mentioned above, we found that eight amino acid residues were different within ATP-binding pockets (Fig. 2c and d and Table 1). Based on this, we designed primers

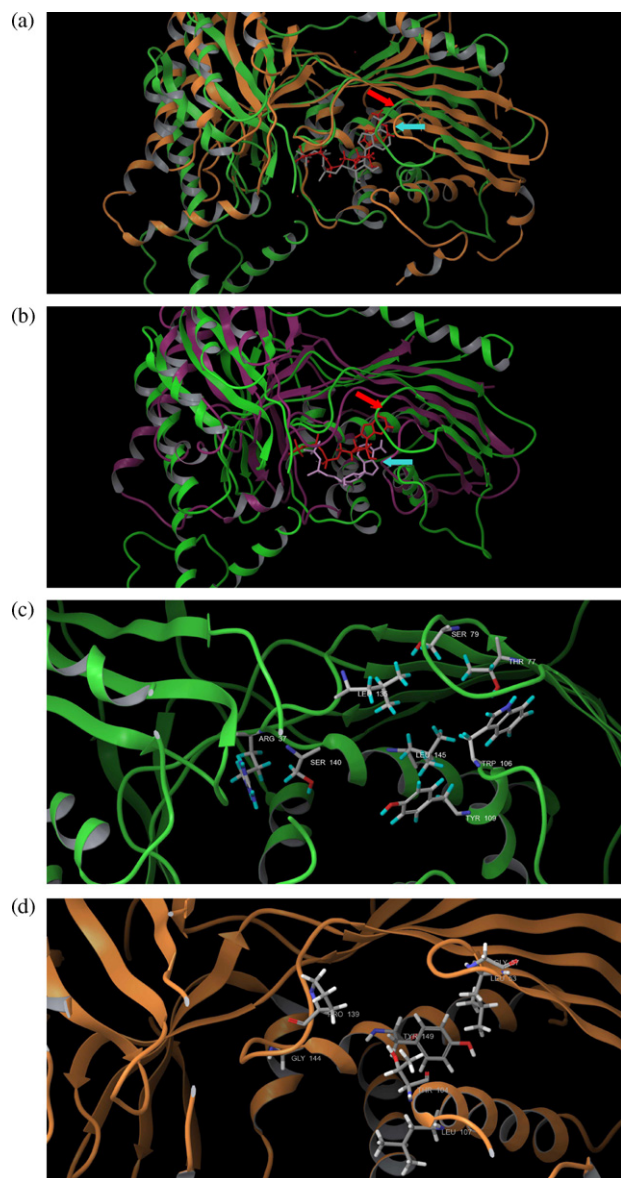
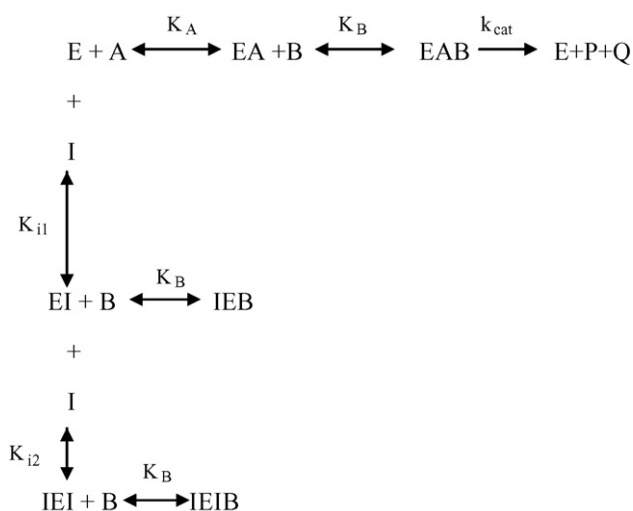


Fig. 2. Crystal structure alignment of GHMP kinases and amino acid residues which are different in ATP-binding pockets of GALK and MVK. (a) Human GALK (1wu, green) aligned with human MVK (1kvk, orange), red arrow: L1 loop of GALK; blue arrow: L1 loop of HSK; AMPPNP in red color was the molecule from GALK structure; ATP in gray color was the molecule from MVK structure. (b) Human GALK (1wu, green) aligned with HSK (1fwk, maroon), red arrow: L1 loop of GALK; blue arrow: L1 loop of HSK; AMPPNP in red color was the molecule from GALK structure; ADP in light purple color was the molecule from HSK structure. (c) Residues which are different in ATP-binding pocket of GALK. (d) Residues which are different in ATP-binding pocket of GALK. (For interpretation of the references to color in this figure caption, the reader is referred to the web version of the article.)

that changed the residues of GALK to corresponding residues of MVK (Table 1). Some of the residues were also changed to alanine.

We expressed these mutated proteins and tested their enzymatic properties. As shown in Table 4, the K_M of ATP for eight of ten active GALK mutants increased and six out of eight increased more than tenfold. This decrease in apparent affinity correlated with the fact that these residues are in the ATP-binding pocket. The K_M for the other two mutants, S140G and R37K, decreased. Four of ten mutant GALK enzymes, T77L, S79N, Y109L and GALK Loop to MVK Loop, had an increased K_M for galactose, but they are all less than fivefold. All k_{cat} of the mutants decreased except Y109L, which increased more than twofold. Among all active GALK mutants, the



Scheme 1. Parabolic competitive inhibition.

one that has its L1 loop changed had the worst effects, both the K_M for galactose and ATP increased the most and k_{cat} decreased the most.

Surprisingly, none of the mutations affected the IC_{50} of compound 1. One mutation, S140G, increased the IC_{50} of compounds 4 and 24. Although the L1 loop is the most noticeable structural difference of these two closely related enzymes, and the substitution of this loop significantly impaired GALK activity, it did not affect IC_{50} of the three inhibitory molecules with human GALK. Ser¹⁴⁰ of GALK resides at the signature motif of the GHMP kinase family, Motif II, but this amino acid is not conserved among the GHMP kinases and GALK is the only member that has a serine at this site. This could explain the selectivity of compounds 4 and 24 for GALK (see Table 3). As for compound 1, we cannot postulate which residue or residues confer its selectivity for GALK relative to the other GHMP kinases based on the site-directed mutagenesis data.

3.4. Kinetic studies of the compounds

We analyzed the kinetics of inhibition by compounds 1, 4 and 24. Human GALK catalyzes the reaction in an ordered mechanism which first binds ATP and then galactose [26]. If the galactose concentration were held at saturated levels (1.5 mM) and the ATP concentration were varied, compound 1 showed an unique inhibitory pattern known as parabolic inhibition (Fig. 3a and b). As shown in Fig. 3, the K_M^{app}/V_M^{app} increased nonlinearly as the concentration of the inhibitor increased: at higher compound concentrations the K_M^{app}/V_M^{app} increased dramatically compared with these kinetic parameters at lower concentrations. Since the $1/V_M^{app}$ did not change, compound 1 was regarded as a parabolic competitive inhibitor of ATP and described as Scheme 1 and Eq. (1).

Four equations can be derived from the above scheme, which represent parabolic competitive inhibition:

$$V_0 = \frac{V_M AB}{K_A(K_B + IK_B/K_{i1} + I^2 K_B/K_{i1}K_{i2} + IB/K_{i1} + I^2 B/K_{i1}K_{i2}) + A(K_B + B)} \quad (1)$$

$$K_M^{app} = K_A \frac{(K_B + IK_B/K_{i1} + I^2 K_B/K_{i1}K_{i2} + IB/K_{i1} + I^2 B/K_{i1}K_{i2})}{K_B + B} \quad (2)$$

$$\frac{1}{V_M^{app}} = \frac{K_B + B}{V_M} \quad (3)$$

$$\frac{K_M^{app}}{V_M^{app}} = K_A \left(\frac{K_B + IK_B/K_{i1} + I^2 K_B/K_{i1}K_{i2} + IB/K_{i1} + I^2 B/K_{i1}K_{i2}}{V_M} \right) \quad (4)$$

Table 4Effect of amino acid changes in human GALK on their enzymatic properties and the IC₅₀ of inhibitors 1, 4 and 24.

Mutations	k_{cat} (S ⁻¹)	K_M of ATP (μM)	K_M of galactose (μM)	Effects on IC ₅₀ of compound 1	Effects on IC ₅₀ of compound 4	Effects on IC ₅₀ of compound 24
T77L	4.1	218.4	1305.2	None	None	None
S79N	4.8	303.4	1227.3	None	None	None
L145Y	11.6	259.7	222.7	None	None	None
L145A	6.4	379.9	356.8	None	None	None
W106A	No protein expression	–	–	–	–	–
W106T	No protein expression	–	–	–	–	–
Y109L	43.2	70.2	963.2	None	None	None
Y109A	8.7	579.3	268.7	None	None	None
GALK Loop to MVK Loop	0.1	695.4	1857.3	None	None	None
S140G	2.1	8.2	141.9	None	Increased tenfold	Increased twentyfold
L135P	13.3	51.1	544.9	None	None	None
R37K	0.4	6.4	623.8	None	None	None
R37A	No activity	–	–	–	–	–
WT	17.5	20.9	319	–	–	–

Eqs. (2)–(4) define the results shown in Fig. 1a and b in which $K_M^{\text{app}}/V_M^{\text{app}}$ increased parabolically when compound 1 increased and $1/V_M^{\text{app}}$ was kept constant.

If Eq. (1) were rearranged according to B, where ATP was at a saturated level with varying galactose concentration, then we will have the followings:

$$V_0 = \frac{V_m \text{ AB}}{K_B(K_A + A + I K_A/K_{i1} + I^2 K_A/K_{i1}K_{i2}) + B(A + I K_A/K_{i1} + I^2 K_A/K_{i1}K_{i2})} \quad (5)$$

and

$$K_M^{\text{app}} = K_B \left(\frac{K_A + A + I K_A/K_{i1} + I^2 K_A/K_{i1}K_{i2}}{A + I K_A/K_{i1} + I^2 K_A/K_{i1}K_{i2}} \right) \quad (6)$$

$$\frac{1}{V_M^{\text{app}}} = \frac{A + I K_A/K_{i1} + I^2 K_A/K_{i1}K_{i2}}{V_m} \quad (7)$$

When we performed the experiments, ATP level was saturated; As a result, A was much larger than K_A , so $K_A + A + I K_A/K_{i1} + I^2 K_A/K_{i1}K_{i2} \approx A + I K_A/K_{i1} + I^2 K_A/K_{i1}K_{i2}$. K_M^{app} could be regarded as constant and $1/V_M^{\text{app}}$ increased parabolically as inhibitor concentration increased just as shown in Fig. 3c and d. These results confirmed that the assumption of Scheme 1 was correct and compound 1 was a parabolic competitive inhibitor for GALK.

The kinetic results for compounds 4 and 24 indicated that they are typical mixed inhibitors for GALK as shown in Fig. 3e–h. The unusual behavior of compound 1 may explain the reason why changes of amino acids at the presumptive ATP-binding site of GALK did not reveal any specific residues that interacted with this compound, as it probably has two binding sites for GALK. The sperm-specific isozyme of lactate dehydrogenase (LDH-C4) also exhibited “parabolic mixed-type” inhibition by gossypol [27]. The kinetic data and site-directed mutagenesis data of compounds 4 and 24 are consistent and suggest that these two inhibitors interact with the same amino acid residue in GALK and inhibit the enzyme by similar mechanisms.

3.5. Docking of compounds to GALK

Based on the information from site-directed mutagenesis and kinetic studies, we used a molecular docking program to generate possible binding models for compounds 4 and 24. Docking programs have been applied widely in drug development for virtual screening of enzyme inhibitors and predicting interactions of compounds and target proteins. Among the software programs cited in literature, GLIDE (Schrödinger, LLC, New York) is regarded as one of the best [28].

The protein structure we used was human GALK protein co-crystallized with galactose and the ATP analogue AMPPNP (PDB: 1wu). First, we evaluated the software by self-dockings: Galactose and AMPPNP were docked back to the protein structure which was already prepared as mentioned in the methods section. The docking poses of galactose and AMPPNP were identical to the poses determined in the crystal structure (data not shown). The root mean square deviations (RMSD) between docked poses and crystal structure were less than 1.5 Å for both galactose and AMPPNP. These results supported our desire to use the GLIDE docking program for further virtual modeling.

Next, compounds 4 and 24 were prepared and docked to the virtual protein structure. At first, we did not set any bond constraints for the docking exercises. Surprisingly, both compounds 4 and 24 did not form interactions with Ser¹⁴⁰ as suggested from the site-directed mutagenesis data. Instead, they formed hydrogen bonds with the hydroxyl group of Ser¹⁴¹ which is conserved among the GHMP kinase family (Fig. 4c and d). Interestingly, the structures of GALK and MVK associated with this site are nearly identical and the two serines of GALK and MVK at position 141 overlapped. It is highly unlikely that the change from serine to glycine at amino acid-140 of GALK would cause any significant change of Ser¹⁴¹. Also, as shown in Fig. 4c and d, the two compounds were close to other residues in the mutagenesis studies and if these docking poses are correct, it is likely that some of these mutations in these residues will affect the binding of these two compounds. Yet, the results from our site-directed mutagenesis experiments did not support this hypothesis. Further, since these two compounds appeared to dock to the middle of ATP-binding site in these docking poses, they should act as ATP competitive inhibitors, instead of mixed inhibitors as shown in our kinetic studies. Then we performed the docking experiments again with constraints that the compounds need to form interactions with Ser¹⁴⁰. The new binding models are shown in Fig. 4a and b. For compound 4, as shown in Fig. 4a, two dione oxygen atoms of these compounds faced residue Ser¹⁴⁰, and form hydrogen bonds with the hydroxyl group and the backbone hydrogen atom of Ser¹⁴⁰. More importantly, the docking pose of compound 4 did not interact with other residues included in the mutagenesis studies such as Tyr¹⁰⁹, Leu¹⁴⁵, Thr⁷⁷, Ser⁷⁹ and Leu¹³⁵. These GALK mutations did not affect the binding affinity of compound 4. Also, the docking site which compound 4 occupied was close to the ATP-binding site, which explained its mixed competition to ATP determined by the kinetic studies (Fig. 3e and f).

Since the binding affinity of compound 24 was affected by the same amino acid residue, Ser¹⁴⁰, as compound 4, it is reasonable that the docking pose of compound 24 also formed hydrogen bond with the hydroxyl hydrogen of Ser¹⁴⁰, as shown in Fig. 4b. In

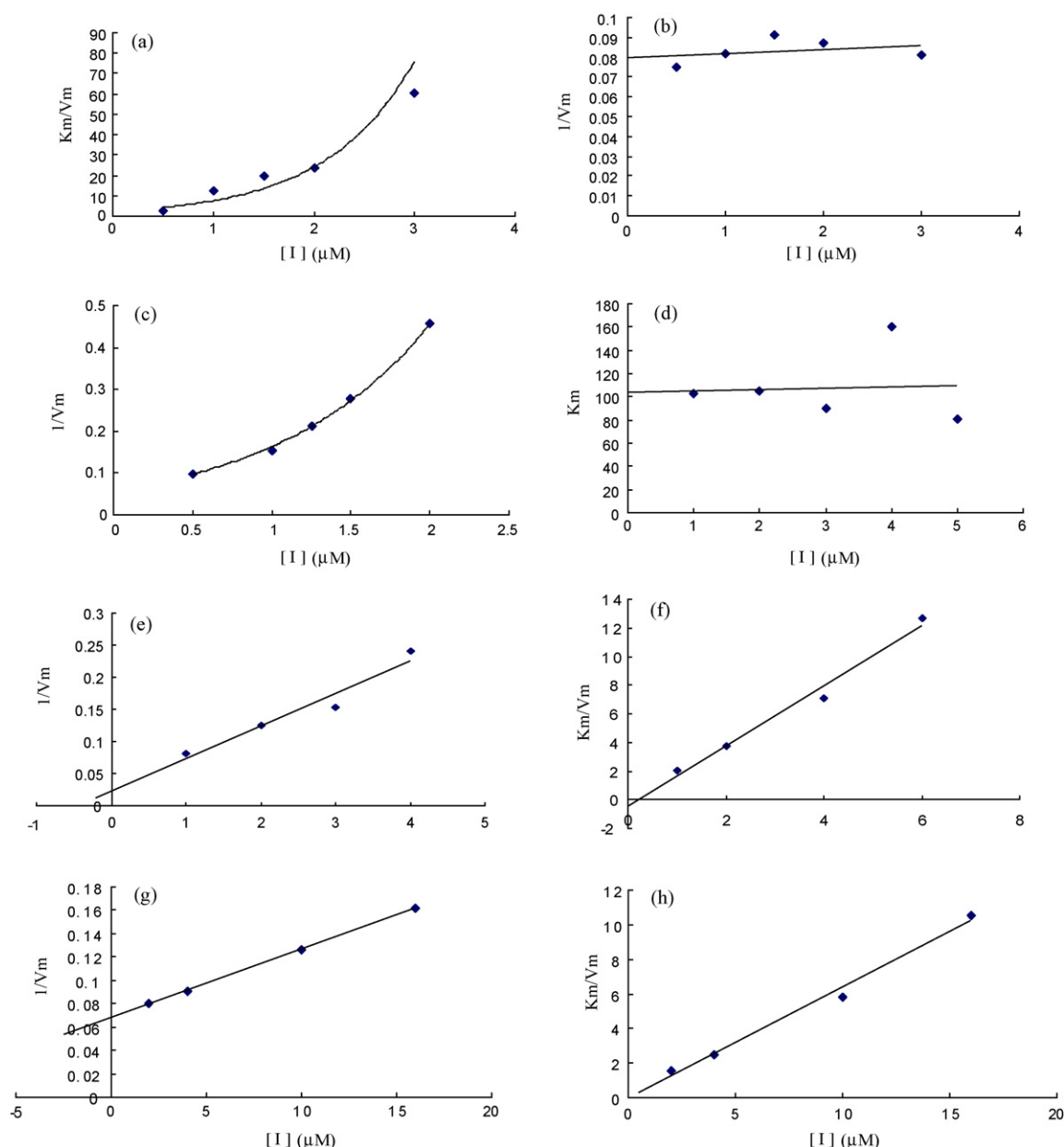


Fig. 3. Enzymatic study of compounds. Enzyme inhibition by compounds 1, 4 and 24 were tested under saturated galactose and varied ATP concentration (a, b, e–h) or saturated ATP and varied galactose concentration (c and d). Triplicate data were analyzed with Sigma Plot 10.0 software. a. Plot of K_m/V_{\max} vs. compound 1 concentration when galactose was saturated and ATP varied. (b) Plot of $1/V_{\max}$ vs. compound 1 concentration under the same condition as a. (c) Plot of $1/V_{\max}$ vs. compound 1 concentration when ATP was saturated and galactose varied. (d) Plot of K_m vs. compound 1 concentration under the same condition as c. (e) Plots of $1/V_{\max}$ vs. compound 4 concentration under the same condition as a. (f) Plot of K_m/V_{\max} vs. compound 4 concentration under the same condition as a. (g) Plot of $1/V_{\max}$ vs. compound 24 concentration under the same condition as a. (h) Plot of K_m/V_{\max} vs. compound 24 concentration under the same condition as a.

addition, this docking model indicated that compound 24 formed extensive hydrogen bond interactions with other residues: Arg²²⁸, Glu¹⁷⁴, Tyr²³⁶, Ser¹⁴² and Arg¹⁰⁵. Again, compound 24 had no interaction with other residues included in the mutagenesis studies. Similar to compound 4, compound 24 occupied the ATP phosphate-binding domain and the area close to the catalytic center, which might also explain its mixed inhibition as shown in kinetic studies (Figs. 4d and 3g and h).

3.6. Lowering Gal-1-P in primary and transformed fibroblasts

Earlier attempts to lower intracellular Gal-1-P concentrations in cultured diploid primary GALT-deficient fibroblasts challenged with galactose were not successful due to the inherent toxicity

of compounds (data not published). This motivated us to try an SV40-transformed GALT-deficient fibroblast cell line, GM00638A, which was more robust in culture and tolerant to compounds 1 and 24. These cells remain viable in the presence of 10 μM of compounds 1 and 30 μM of compound 24. More importantly, these GALT-deficient cells accumulated Gal-1-P upon galactose challenge (Fig. 5a and b). When treated with compound 1, there was a dose-dependent effect of this GALK inhibitor on Gal-1-P accumulation. At an external concentration of 6 μM , Compound 1 lowered intracellular Gal-1-P to a level that approached that of the non-treated control (Fig. 5a). Similarly, treatment of compound 24 at 20 μM decreased the accumulation of Gal-1-p by 70% as compared to the positive control (Fig. 5b). This is the proof-of-concept data that small molecule inhibitors of GALK can lower Gal-1-P

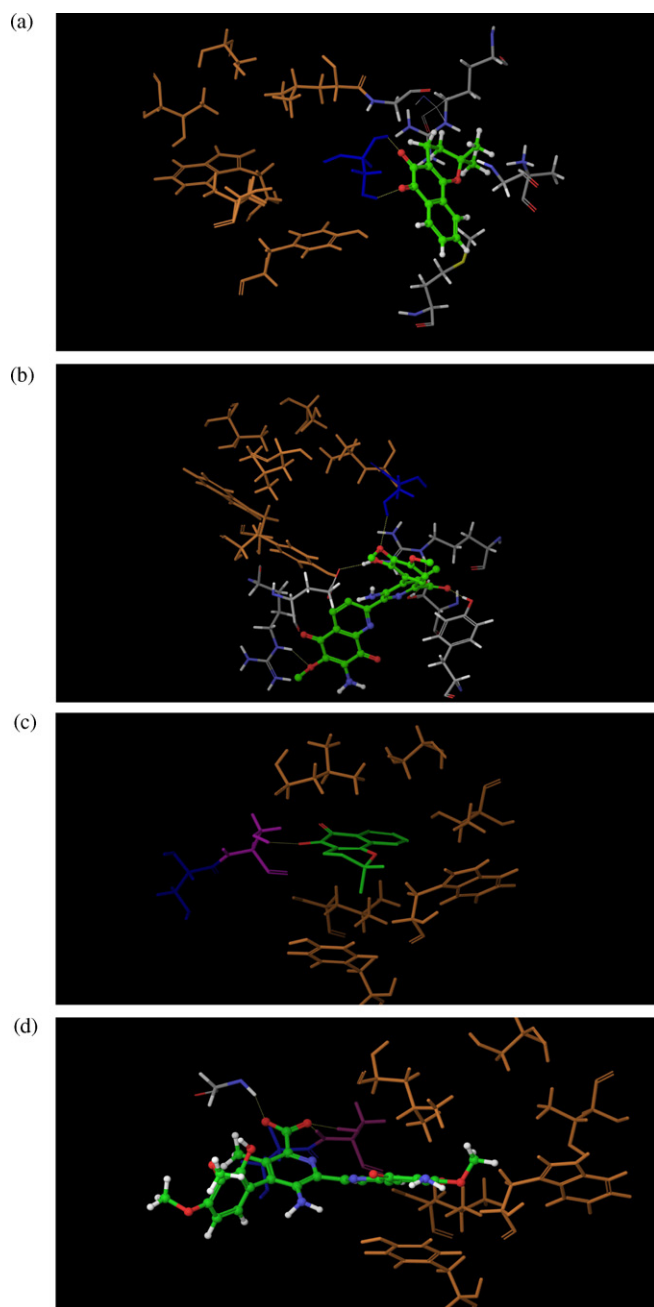


Fig. 4. Docking of compounds 4 and 24 to GALK (1wu). Docking of compound 4 (a and c) and 24 (b and d) to GALK, with constraints (a and b) and without constraints (c and d). Molecules in green are compounds. Ser¹⁴⁰ is in dark blue, Ser¹⁴¹ is in purple, other residues of the site-directed mutagenesis studies are in yellow. Other residues surrounding the compounds are in gray. Yellow dot lines are hydrogen bond formed between the compounds and protein. (For interpretation of the references to color in this figure caption, the reader is referred to the web version of the article.)

in galactose-challenged GALT-deficient cells. Unfortunately, long-term exposure of these first-generation GALK inhibitors was too toxic for diploid cells. The kinetic and structural interactions of this first group of selective GALK inhibitors will, however, enable future development of non-toxic and more specific GALK inhibitors.

4. Discussion

Elevated concentrations of Gal-1-P in GALT-deficient cells is considered the major culprit of chronic, organ-specific dysfunction in patients with Classic Galactosemia. As Gal-1-P is the product

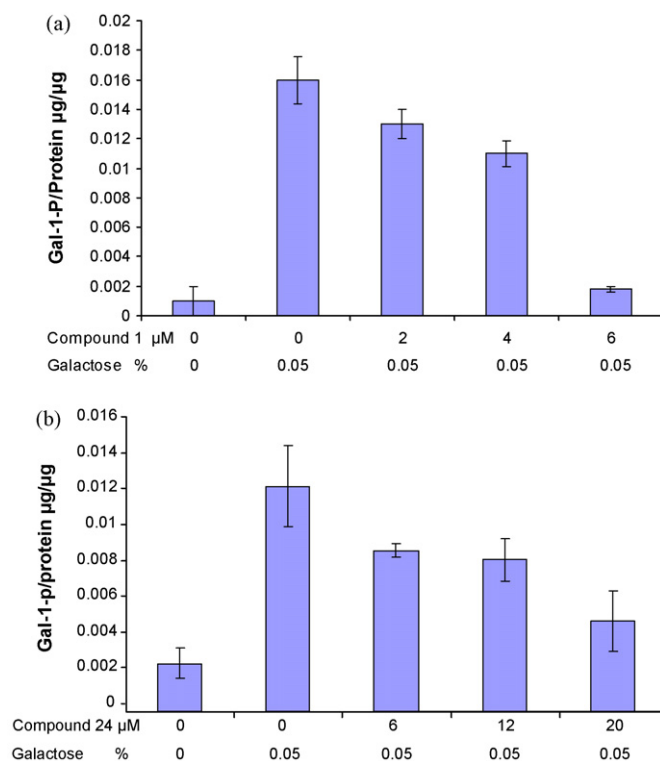


Fig. 5. Gal-1-P level upon compounds 1 and 24 treatment in GM00638A Gal-1-p levels were measured after the cells were treated with compound for 4 h with increasing concentration and then challenged with 0.05% galactose. Cells in glucose served as negative control.

of galactokinase (GALK), at least four groups of investigators proposed to inhibit the GALK enzyme with specific, non-toxic, low molecular weight compounds as a rational and novel approach to treat Classic Galactosemia [18,29–31]. We are aware of the suggested possibility that some of the GALK inhibitors might also inhibit *N*-acetylgalactosamine kinase (GALK2) due to the structural similarity [32], and potentially impair the biosynthesis of *N*-acetylgalactosamine-1-phosphate—an important intermediate in the biosynthesis of UDP-*N*-acetylgalactosamine. However, as UDP-galactose 4-epimerase (GALE) catalyzes the interconversion between UDP-*N*-acetylgalactosamine and UDP-*N*-acetylglucosamine [33], any inhibition of GALK2 is unlikely to result in deficiency of UDP-*N*-acetylgalactosamine. To date, our group has screened different chemical compound libraries composed of about 50,000 small molecules with diverse structural scaffolds for their inhibitory properties against activity of purified GALK. Thus far, we have identified nearly 150 small molecules (or hits) that inhibited human GALK activity *in vitro* at the level of 86.5% or more [18]. We selected 34 of these compounds for further characterization in this study. For the first time, we demonstrated the reduced accumulation of Gal-1-P in GALT-deficient cells treated with two small molecule compounds (compounds 1 and 24) selectively inhibiting GALK (Fig. 5). This is a proof-of-concept that stronger, non-toxic, and more specific small molecule GALK inhibitors might provide adjunct therapy for patients with Classic Galactosemia. Nevertheless, we must recognize that like most drug discovery projects, the identification of these first-generation lead compounds only marks the beginning of a long journey of drug development. To optimize these lead compounds and make them applicable as therapeutics in the future, one must thoroughly characterize them with respect to their potency (Table 2), modes of inhibition (Fig. 3), selectivity/toxicity profiles (Table 3), and interactions with the GALK target at the structural level (Fig. 4).

Yet, one must not assume that the characterization of these inhibitors is only useful for the discovery of more potent and safe therapeutics. In fact, as we showed in this study, the characterization process also offers novel insights into the fundamental knowledge on the structure-functions of GALK and other members of the GHMP kinases. For instance, the lack of cross-inhibition for nearly all GALK inhibitors identified for the highly conserved glucokinase and hexokinase confirmed the fact that despite GALK phosphorylates galactose, it is remotely related to the members of the sugar kinase family (Table 3). As we examined the selectivity profiles of the GALK inhibitors against other closely related GHMP kinases, we identified six compounds that uniquely inhibited GALK (Table 3). Although these results were not entirely unexpected, we were intrigued by them, especially after we compared the crystal structures of human GALK and human MVK (Fig. 2). From Fig. 2, it is clear that the active sites of these two closely related GHMP kinases are highly similar, which is not surprising as human GALK and human MVK shared 70 identical residues and 69 conserved residues. So what are the structural determinants of the two GHMP kinases giving rise to the observed selectivity of the GALK inhibitors? We decided to address this fundamental question with site-directed mutagenesis experiments and computer modeling.

From our initial structural analysis, the difference in size of the L1 loops in human GALK and human MVK became obvious and presented a logical explanation for the difference in the selectivity of inhibitors towards the two closely related GHMP kinases (Fig. 2a and b). However, further investigation revealed that this was not the case. Although this loop affects the GALK activity, maybe through affecting ATP binding, it did not appear to interact with the compounds we tested here (Table 4). Through site-directed mutagenesis, we altered the non-conserved amino acids at the ATP-binding site of GALK and re-tested the inhibitors with the resulting variant GALK proteins. We found that one amino acid residue, Ser¹⁴⁰, conferred the selectivity for two compounds of interest, compound 4 and 24, respectively. Using this knowledge, we then generated binding models of these two compounds with the high-precision docking program called GLIDE (Schrödinger, LLC New York, 2009). The virtual models correlated with the actual results from site-directed mutagenesis and kinetic studies, and gave us the first impression of how these inhibitors might interact with GALK. One interesting observation is that the residue, Ser¹⁴⁰, and the computer models indicated that the selectivity of these two compounds for GALK was conferred by the area near the phosphate-binding region, while in protein kinases the two hydrophobic regions close to adenine binding region and the sugar-binding pocket often determine the selectivity of kinase inhibitors [34].

The most potent inhibitor identified from high-throughput screening, compound 1, inhibited GALK as a parabolic competitive inhibitor as shown in kinetic studies (Fig. 3a–d). This suggested there are two binding sites for compound 1 in the GALK protein. We could not identify specific residue interacts with this compound and therefore, we could not confirm a binding model. Interestingly, the structures of compounds 1 and 4 are very similar. Compound 1 is a derivative of dioxophenanthren and compound 4 is very similar to dioxophenanthren except it has a nitro substitution. Yet they behave so differently with regard to GALK inhibition.

In conclusion, we identified three compounds which selectively inhibited GALK with high potency, and illustrated the inhibition modes of these compounds to GALK. Moreover, through site-directed mutagenesis we identified one amino acid residue required for the inhibitory function of two of the three selective compounds. Based on these results, we generated binding models of these two compounds using a high-precision docking program. Lastly, we showed for the first time two of the GALK inhibitor prevented Gal-1-P accumulation in galactose-challenged GALT-deficient cells.

Conflict of interest

None declared.

Acknowledgements

Research grant support to Kent Lai includes NIH grant 5R01 HD054744-04, 5R01 HD054744-04S1 and 7R03 MH085689-02.

References

- [1] L.F. Leloir, The enzymatic transformation of uridine diphosphate glucose into a galactose derivative, *Arch. Biochem.* 33 (2) (1951) 186–190.
- [2] K.J. Isselbacher, et al., Congenital galactosemia, a single enzymatic block in galactose metabolism, *Science* 123 (3198) (1956) 635–636.
- [3] R. Gitzelmann, H.C. Curtius, I. Schneller, Galactitol and galactose-1-phosphate in the lens of a galactosemic infant, *Exp. Eye Res.* 6 (1) (1967) 1–3.
- [4] K. Lai, et al., GALT deficiency causes UDP-hexose deficit in human galactosemic cells, *Glycobiology* 13 (4) (2003) 285–294.
- [5] F.C. Sitzmann, H. Kaloud, [Congenital disorders of galactose metabolism], *Med. Klin.* 70 (12) (1975) 491–498.
- [6] O.M. Rennert, Disorders of galactose metabolism, *Ann. Clin. Lab. Sci.* 7 (6) (1977) 443–448.
- [7] K. Dogan, et al., [Inborn disorders of galactose metabolism: report of a case of “classical galactosemia” (author’s transl)], *Lijec Vjesn* 99 (10) (1977) 589–594.
- [8] C.I. Kaye, et al., Newborn screening fact sheets, *Pediatrics* 118 (3) (2006) pe934–pe963.
- [9] G.T. Berry, et al., The effect of dietary fruits and vegetables on urinary galactitol excretion in galactose-1-phosphate uridylyltransferase deficiency, *J. Inherit. Metab. Dis.* 16 (1) (1993) 91–100.
- [10] P.B. Acosta, K.C. Gross, Hidden sources of galactose in the environment, *Eur. J. Pediatr.* 154 (7 Suppl. 2) (1995) S87–92.
- [11] G.T. Berry, et al., Endogenous synthesis of galactose in normal men and patients with hereditary galactosaemia, *Lancet* 346 (8982) (1995) 1073–1074.
- [12] G.T. Berry, et al., The rate of de novo galactose synthesis in patients with galactose-1-phosphate uridylyltransferase deficiency, *Mol. Genet. Metab.* 81 (1) (2004) 22–30.
- [13] R. Gitzelmann, Letter: additional findings in galactokinase deficiency, *J. Pediatr.* 87 (6 Pt 1) (1975) 1007–1008.
- [14] D. Stambolian, et al., Cataracts in patients heterozygous for galactokinase deficiency, *Invest. Ophthalmol. Vis. Sci.* 27 (3) (1986) 429–433.
- [15] R. Gitzelmann, H.J. Wells, S. Segal, Galactose metabolism in a patient with hereditary galactokinase deficiency, *Eur. J. Clin. Invest.* 4 (2) (1974) 79–84.
- [16] H.C. Douglas, D.C. Hawthorne, Enzymatic expression and genetic linkage of genes controlling galactose utilization in *Saccharomyces*, *Genetics* 49 (1964) 837–844.
- [17] H.C. Douglas, D.C. Hawthorne, Regulation of genes controlling synthesis of the galactose pathway enzymes in yeast, *Genetics* 54 (3) (1966) 911–916.
- [18] K.J. Wierenga, et al., High-throughput screening for human galactokinase inhibitors, *J. Biomol. Screen.* 13 (5) (2008) 415–423.
- [19] P. Bork, C. Sander, A. Valencia, Convergent evolution of similar enzymatic function on different protein folds: the hexokinase, ribokinase, and galactokinase families of sugar kinases, *Protein Sci.* 2 (1) (1993) 31–40.
- [20] P. Bork, C. Sander, A. Valencia, An ATPase domain common to prokaryotic cell cycle proteins, sugar kinases, actin, and hsp70 heat shock proteins, *Proc. Natl. Acad. Sci. U.S.A.* 89 (16) (1992) 7290–7294.
- [21] K. Lai, A.C. Willis, L.J. Elsas, The biochemical role of glutamine 188 in human galactose-1-phosphate uridylyltransferase, *J. Biol. Chem.* 274 (10) (1999) 6559–6566.
- [22] R.A. Friesner, et al., Glide: a new approach for rapid, accurate docking and scoring. 1. Method and assessment of docking accuracy, *J. Med. Chem.* 47 (7) (2004) 1739–1749.
- [23] T.A. Halgren, et al., Glide: a new approach for rapid, accurate docking and scoring. 2. Enrichment factors in database screening, *J. Med. Chem.* 47 (7) (2004) 1750–1759.
- [24] R.A. Friesner, et al., Extra precision glide: docking and scoring incorporating a model of hydrophobic enclosure for protein-ligand complexes, *J. Med. Chem.* 49 (21) (2006) 6177–6196.
- [25] M.A. Larkin, et al., Clustal W and Clustal X version 2.0, *Bioinformatics* 23 (21) (2007) 2947–2948.
- [26] F.J. Ballard, Kinetic studies with liver galactokinase, *Biochem. J.* 101 (1) (1966) 70–75.
- [27] D.T. Stephens, et al., Kinetic characterization of the inhibition of purified cynomolgus monkey lactate dehydrogenase isozymes by gossypol, *J. Androl.* 7 (6) (1986) 367–377.
- [28] M. Michino, et al., Community-wide assessment of GPCR structure modelling and ligand docking: GPCR Dock 2008, *Nat. Rev. Drug. Discov.* 8 (6) (2009) 455–463.
- [29] A.M. Bosch, Classical galactosaemia revisited, *J. Inherit. Metab. Dis.* 29 (4) (2006) 516–525.

- [30] D.J. Timson, GHMP kinases—structures, mechanisms and potential for therapeutically relevant inhibition, *Curr. Enzyme Inhib.* 3 (1) (2007) 77–94.
- [31] J. Fridovich-Keil, Toward Improved Intervention for Classic Galactosemia. <http://www.galactosemia.org/PGC.awards.asp>, 2007.
- [32] A. Agnew, D. Timson, Mechanistic studies on human N-acetylgalactosamine kinase, *J. Enzyme Inhib. Med. Chem.* (2009).
- [33] J.B. Thoden, et al., Molecular basis for severe epimerase deficiency galactosemia. X-ray structure of the human V94m-substituted UDP-galactose 4-epimerase, *J. Biol. Chem.* 276 (23) (2001) 20617–20623.
- [34] M. Cherry, D.H. Williams, Recent kinase and kinase inhibitor X-ray structures: mechanisms of inhibition and selectivity insights, *Curr. Med. Chem.* 11 (6) (2004) 663–673.